Manipulation of electron flow using near-zero index semiconductor metamaterials

Romain Fleury and Andrea Alù*

Department of Electrical & Computer Engineering, The University of Texas at Austin, Austin, TX 78712, USA

(Received 16 May 2014; revised manuscript received 15 July 2014; published 29 July 2014)

We study the possibility of controlling the propagation of ballistic electrons using an electronic metamaterial with zero quantum index of refraction. This is obtained by tailoring the band structure of a semiconductor superlattice to exhibit a Dirac cone at the center of the Brillouin zone, creating an artificial quantum medium with zero refractive index for electrons. We demonstrate attractive functionalities, such as anomalous tunneling, ideal matching, electronic routing, cloaking, and focusing. We envision applications in nanoelectronics and sensing.

DOI: 10.1103/PhysRevB.90.035138 PACS number(s): 73.63.−b, 78.67.Pt, 85.30.−z

I. INTRODUCTION

Over the last century, the dramatic development of solid-state physics and technology has enabled a new level of control over electron motion in crystalline solids, leading to a wealth of fascinating applications with a tremendous impact on our society, associated to the development of information sciences and consumer electronics. At the basis of this scientific revolution is the understanding of particle dynamics in periodic potentials, which has made possible the engineering of a plethora of semiconductor materials and devices, and enlarged our ability to tame electron flow for coding, transmitting, and processing information. With the recent development of nanoscience and technology, the characteristic length of electronic components has considerably shrunk, and researchers are currently facing new challenges related to the manipulation and control of ballistic electrons at the nanoscale.

In an unrelated field of research, metamaterials have fostered research interest for more than a decade now, supporting anomalous wave propagation functionalities that fundamentally differ from any other known natural material [1]. These artificial materials possess peculiar properties, not readily available in nature, like negative [2], very low [3–14], or very large [15] constitutive parameters. They retain their exotic response from their subwavelength structure, rather than from the intrinsic properties of the materials they are built of. Metamaterials have provided new ways to manipulate waves at the subwavelength scale, enabling subwavelength focusing [16,17], phase shaping [4,13], polarization control [18], giant nonreciprocity [19,20], boosted radiation [12,21], and cloaking [22–27].

Notwithstanding fundamental differences in their physical properties, like statistics, mass, and spin, electrons and photons are formally similar in their propagation properties, due to the wave-particle duality [28]. The wave function of an electron, representing the amplitude of its probability of presence, follows a wave equation, the Schrodinger equation, just like electromagnetic waves, which propagate according to Maxwell equations. Extending this analogy further to the propagation of these two types of waves in materials, it is natural to associate intrinsic semiconductors to natural optical materials, and photonic crystals, which are made of a mesoscopic periodic arrangement of natural materials, to quantum superlattices. Semiconductor superlattices operated near their Γ point (i.e., in the long-wavelength limit) can in this sense be viewed as quantum metamaterials [29].

A few pioneering works have recently started investigating what the metamaterial concepts can bring to semiconductor physics and electronic applications. Superlattices with engineered band structures were envisioned long before the development of metamaterials [30], but looking at them as quantum metamaterials may enable the transposition of the most exciting metamaterial-related possibilities. One of the most famous applications of double-negative metamaterials, subwavelength focusing, has been discussed in some early works for electrons [31,32] and recently translated to matter waves from the theoretical standpoint [33,34]. Cloaking from matter waves has been theoretically predicted with cloaks made out of layers of quantum metamaterials with specifically tailored effective mass and potential [35–41]. Quantum metamaterials were also proposed to realize superconducting structures [42–45], or to tailor the mobility of electrons and overcome the usual speed limitations of standard integrated circuits and optical devices [46,47]. A homogenization theory was also introduced to rigorously describe the propagation of matter waves in periodic potentials using an averaged effective Hamiltonian depending on two effective parameters (mass and potential) [48]. This effective-medium theory was shown to be particularly relevant for describing propagation of matter waves in mesoscopic structures such as superlattices, and to be closely related to the Bastard envelope function theory [49].

In this paper, we further expand the quantum reach of metamaterial science by demonstrating the unusual properties of a semiconductor metamaterial with zero refractive index for electrons. We show that a properly designed superlattice made of conventional semiconductors can support a zero refractive index for electrons, at a specific design energy. We investigate the use of this quantum metamaterial as a tool to mold the flow of ballistic electrons by shaping the propagation of their wave function and controlling their tunneling properties. After briefly presenting our design, we demonstrate that the proposed material has a zero refractive index for electronic matter waves and it is at the same time impedance matched to its substrate. These unique properties open a plethora of exciting applications, inspired by the anomalous properties of zero-index optical metamaterials [3–9,21]. As a first example, we show in the following that this zero-index metamaterial may be used to arbitrarily connect quantum wires, and tunnel electrons between them, even if the junction is not straight

*alu@mail.utexas.edu

or it presents defects such as sharp twists and bends. This may be used in nanoelectronic systems to connect different subsystems without scattering between them. As a second application, we show how the same metamaterial may be used to suppress the presence of an obstacle, making it invisible in terms of scattering to an incoming electron beam. This peculiarity may be exploited to cloak quantum sensors, defects, or other subsystems from the flow of electrons. Finally, we show how this same quantum metamaterial may be used to focus and defocus electron beams, which may find application in quantum information processing or sensing.

II. A ZERO INDEX QUANTUM METAMATERIAL

Zero index metamaterials were first proposed for electromagnetic waves and studied for their anomalous tunneling and phase-front shaping properties [3–14]. They may be obtained designing a metamaterial to have either zero permittivity or permeability, and they may be matched to free space by combining geometrical and impedance mismatch [6], or by taking both constitutive parameters down to zero [7]. These materials have recently been obtained also for acoustic waves, exploiting similar principles [14,50,51]. Among the different methods for achieving matched electromagnetic or acoustic zero-index metamaterials, one of them is based on tailoring photonic or phononic crystals to induce a Dirac cone at the center of the Brillouin zone, exploiting accidental degeneracy of different Bloch eigenmodes [13]. For such crystals, an effective-medium representation is adequate near the Dirac frequency, since the latter is located at the Γ point. This is quite different from the case of Dirac fermions in graphene, for which the Dirac points are not accidental, but due to hexagonal symmetry, and occur at the first Brillouin-zone edges, a situation incompatible with homogenization. Using this accidental degeneracy method, Huang *et al.* designed and built a two-dimensional (2D) zero index metamaterial for microwaves using a photonic crystal made of alumina rods in air [13]. Similarly, the same group designed and fabricated a 2D zero index metamaterial for acoustic waves, using a tailored sonic crystal constituted of rubber cylinders in water [50]. Followup studies showed that this interesting concept can be extended to 3D geometries [52].

We now present a semiconductor superlattice analogous to such structures. Consider a square lattice of GaAs rods in an AlAs background, as depicted in the inset of Fig. 1. The lattice constant a is arbitrarily fixed to 14 nm, and r is the rod radius. We model both semiconductors as effective media, in which the envelope of the microscopic wave function propagates according to an averaged Hamiltonian with dispersive effective mass m_{eff} and potential V_{eff}, given by the Bastard equations [48,49],

$$m_{\text{eff}} = m_e\left[1+\frac{E_p}{3}\left(\frac{2}{E-E_v}+\frac{1}{E-E_v+\Delta_{\text{so}}}\right)\right]^{-1}, \qquad (1)$$

and

$$V_{\text{eff}} = E_c. \qquad (2)$$

In the above equations, m_e is the mass of an electron, E_v and E_c are the valence- and conduction-band energy of the semiconductor, Δ_{so} is the spin-orbit splitting and $E_p = 2P^2m_e/\hbar^2$, P is Kane's parameter. We obtain the superlattice band structure by solving the eigenvalue problem

$$H_{\text{eff}}\Psi = -\frac{\hbar^2}{2}\nabla\cdot\left(\frac{1}{m_{\text{eff}}}\nabla\Psi\right)+V_{\text{eff}}\Psi = E\Psi, \qquad (3)$$

where Ψ is the envelope of the microscopic wave function. Note that the effective mass m_{eff} depends on the energy eigenvalue E, consistent with Eq. (1). This dispersion complicates the analytical solution of Eq. (3), which we have solved numerically using the nonlinear eigenvalue solver of the commercially available software COMSOL Multiphysics, enforcing Daniel-Duke boundary conditions at the GaAs/AlAs heterojunction and Bloch boundary conditions at the unit-cell boundaries. Material parameters are taken from Ref. [53].

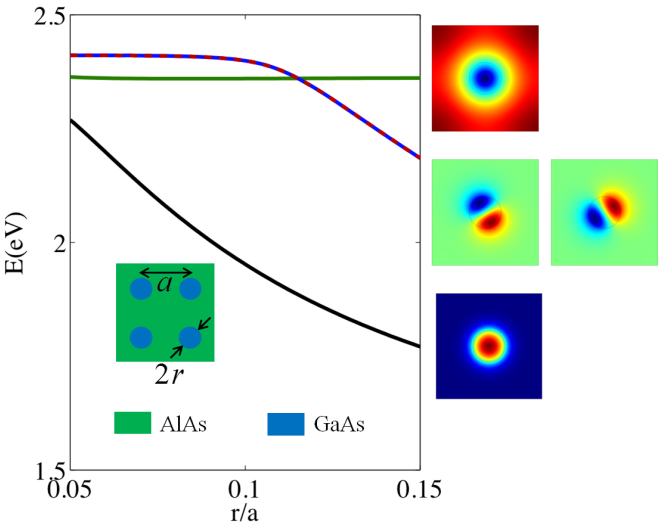

FIG. 1. (Color online) Bloch energy eigenvalues and eigenmodes of the considered square semiconductor superlattice, at the center of the Brillouin zone, for varying values of the filling ratio r/a. Accidental triple degeneracy is obtained for $r/a = 0.115$ and $E = 2.36$ eV between the first doubly degenerate dipolar eigenstate and the second monopolar eigenstate.

In Fig. 1, we show the first three energy eigenvalues at the center of the Brillouin zone ($k = 0$), and look at their evolution when the radius of the GaAs well is varied, at fixed lattice constant $a = 14$ nm. The corresponding eigenmodes are also shown with contour plots representing the real part of the envelope of the electronic wave function. We observe that the structure presents both monopolar and dipolar eigenmodes. The first dipolar mode is doubly degenerate, as expected from the $C4$ symmetry, while the monopolar modes are both nondegenerate. The Bloch eigenvalues all depend on the radius of the wells, but the first monopolar and dipolar bound modes are more sensitive to radius changes than the scattering (unbound) mode, because of the higher value of the wave vector in the GaAs well. This results in a significant redshift of the associated eigenvalues when the radius is increased. Since at sufficiently low values of r the dipolar eigenmodes occur at higher energy than the flat, second monopolar eigenmode, there exists a particular value of r for which these modes experience *accidental* degeneracy. In our particular case, this occurs when $r/a = 0.115$ for $E = 2.36$ eV.

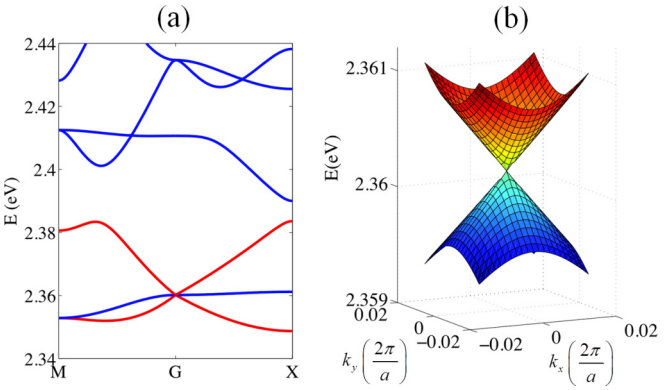

FIG. 2. (Color online) (a) Band diagram of the superlattice for $r/a = 0.115$ for which a Dirac cone is induced at the center of the Brillouin zone (b).

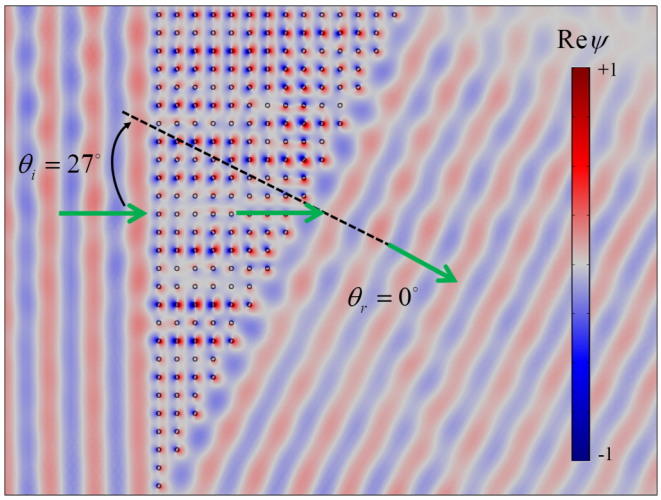

FIG. 3. (Color online) Demonstration of zero index quantum metamaterial. Electrons propagating in the AlAs background are scattered by a prism made of the proposed quantum metamaterial (incidence from the left). At the second interface, the refracted angle is identically zero, unlike the incidence angle, demonstrating that the effective index of the superlattice vanishes at the Dirac cone energy.

To understand the effect of accidental degeneracy on electronic propagation, it is instructing to look at the energy-band diagram of the superlattice. Therefore, we fix $r/a = 0.115$ and look at the Bloch eigenvalues of that particular geometry, further away from the Γ point. The energy-band diagram is reported in Fig. 2(a) along specific paths in the first Brillouin zone, in a small energy window around $E = 2.36$ eV. Figure 2(b) is a 3D representation of the band structure at the degeneracy energy, near the Γpoint. We observe a Dirac cone at the center of the Brillouin zone at the exact energy for which accidental degeneracy was obtained. In addition, the possibility to induce the Dirac cone at the center of the Brillouin zone, where the wave vector approaches zero, enables us to model the superlattice as an effective medium, and to transpose metamaterial concepts to electronic materials. For GaAs well sizes different than $r/a = 0.115$, the superlattice resembles a natural semiconductor, with a band gap around $E = 2.36$ eV, and properties similar in nature to its GaAs and AlAs constituents. It is only when the radius of the GaAs wells gets around this particular value that the band gap closes, and the material band structure is dramatically metamorphosed, mimicking the one of a quasimetal [54–59]. In the following, we demonstrate the potential of such a metamaterial approach in quantum electronics. We indeed show that the structure can operate as a zero-index metamaterial, opening a variety of possibilities for functionalities inherent to metamaterials with near-zero constitutive parameters, establishing the capability of such materials to tame electrons and control their flow.

III. APPLICATIONS AND RESULTS

A direct evidence of the effective zero refractive index and impedance matching of the proposed metamaterial is provided by the simulation in Fig. 3, in which an electronic matter wave propagating in AlAs is incident from the left side of the figure and scattered by a prism made out of the quantum metamaterial. This time-invariant scattering problem is solved numerically, the energy of the electron being set to the Dirac energy. The figure represents a snapshot in time of the real part of the envelope of the quantum wave function. At the first interface with the prism, the electron does not experience any refraction, since it is normally incident. At the second interface, separating the metamaterial from the AlAs background, the angle of refraction is observed to be identically zero such that

$$n \sin\theta_i = 0. \tag{4}$$

Because the angle of incidence θ_i is 27°, Eq. (4) confirms that the quantum refractive index n of our artificial electronic material is zero. In such a material, electrons propagate with infinite phase velocity, and their wave function does not change appreciably even over distances larger than the AlAs de Broglie wavelength, opening interesting possibilities for controlling electrons at the quantum scale. Such a quantum metamaterial is the direct analog of a near-zero index electromagnetic metamaterial, which have indeed been proposed to tailor and mold the phase front of impinging beams [3–11]. Another striking property of this electronic metamaterial is that electrons can penetrate it with little or no reflection from the surrounding AlAs semiconductor. This is best understood within the framework of quantum transmission-line theory [60–64], a simple and accurate method to determine the quantum transmission probability across heterojunctions, that was developed over the past decades as a design tool for resonant tunneling devices [65,66], interference filters [67], and impedance transformers [68]. According to this electron wave optics theory, the generalized transmission-line impedance for any quantum system obeying a time-invariant Schrödinger equation is [60]

$$Z = \frac{\hbar k_z}{i M_{\text{eff}}}, \tag{5}$$

where M_{eff} is the associated effective mass and $\hbar k_z$ the projection of the quasimomentum along the transmission-line direction. In our quantum metamaterial, $\hbar k_z$ can be evaluated from the band diagram of Fig. 2(b), from the linear relation

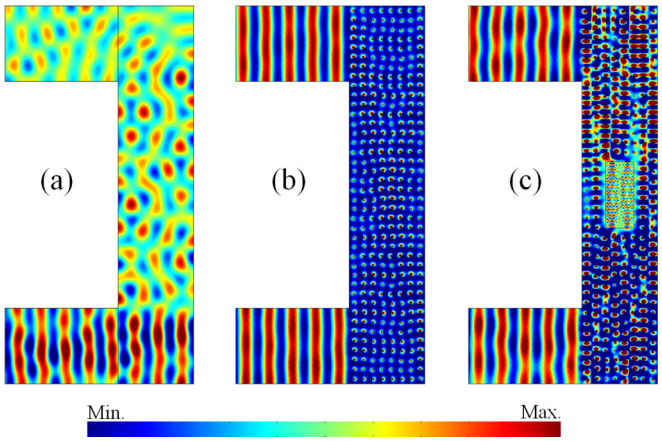

FIG. 4. (Color online) Routing electrons and cloaking obstacles. Electronic flow, incident from the bottom 2D AlAs quantum wire, is significantly disturbed and poorly transmitted to the upper channel when confronted to a 180° turn made out of the same material (a). When connected via the zero index metamaterial (b), electrons teleport through the superlattice with total transmission and no phase shift, as if the space in between were absent. In the presence of a large GaAs obstacle, this exotic tunneling phenomenon remains unaffected, and no collision with the obstacle occurs, demonstrating the cloaking capabilities of the zero effective index semiconductor.

between energy and quasimomentum [48],

$$|E - V_{\text{eff}}| = \hbar k_z v_p, \tag{6}$$

where v_p is an effective Fermi velocity, equal to 58.3 km/s in our case. The homogenized dispersive effective mass of the metamaterial M_{eff} is calculated for zero-band gap semiconductors using the usual formula [48],

$$M_{\text{eff}} = \frac{E - V_{\text{eff}}}{2v_p^2}. \tag{7}$$

Z can be calculated from Eqs. (5)–(7). The reflection coefficient R, ratio of the amplitudes of incident and reflected electronic envelopes at the interface between the AlAs substrate and the quantum metamaterial, is given by the transmission-line formula [69]

$$R = \frac{Z - Z_{\text{AlAs}}}{Z + Z_{\text{AlAs}}}, \tag{8}$$

where Z_{AlAs} is the impedance of the substrate, which can be computed for AlAs from Eqs. (5), (1), and (2). At the Dirac energy, we find $|R|^2 = 3.2\%$, consistent with the almost perfect matching observed in our numerical simulation. The zero-index semiconductor is matched to the AlAs substrate, making it an ideal building block for a new generation of integrated nanodevices. The associated peculiar transmission and refractive properties may be used to our advantage to tame the propagation of ballistic electrons in a novel class of metamaterial-inspired electronic components with unique functionalities.

As a first example of how the zero-index quantum metamaterial may be used for molding electronic motion, consider connecting two misaligned quantum channels, for instance AlAs quantum wires, with a third one. In Fig. 4, we consider a stringent case in which the channels are parallel and we try to force the electron to undergo a U-turn via a third perpendicular channel connecting the ends of the waveguides. Figure 4(a) represents the case where the connecting channel is made of AlAs, just like the other channels. As expected from the abrupt change in direction, the electronic flow is almost completely reflected in the feeding channel. Not only is the probability of finding the electron in the output channel very small, but the electronic flow is totally disturbed and scattered in higher-order modes. In contrast, when the connecting channel is filled by the quantum metamaterial, the electron tunnels through the 180° bend with no reflection, and continues its way undisturbed in the second channel as if the connecting channel was not there and the change of direction had not occurred [Fig. 4(b)]. Because of the near-zero effective index of the metamaterial, the quantum length of the channel $k_z l$ is almost zero, and the electron tunnels through the bend without noticing it, in a quasistatic and reflectionless way. Similar physics occurs in conventional electrical wires at dc, which can indeed be bent and twisted at will without affecting the ability of the connector to carry an electric signal, due to the infinite wavelength. The large phase velocity and impedance matching essentially mimics this effect for electrons at the Dirac energy. This phenomenon is robust to the presence of obstacles and defects in the metamaterial, which are effectively cloaked from the electronic flow. In Fig. 4(c), indeed, we show the case of

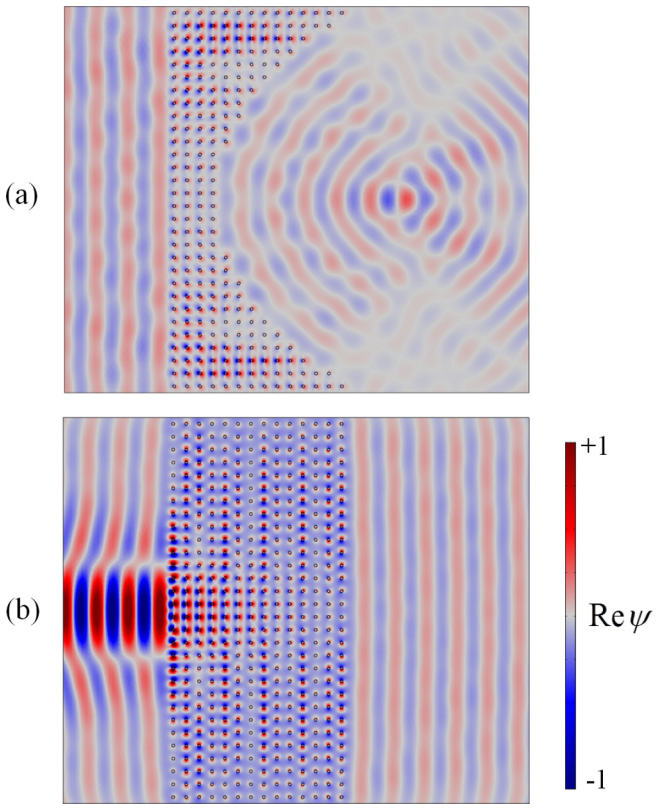

FIG. 5. (Color online) Focusing and defocusing. In panel (a), a plane electronic matter wave is focused by a lens made of our zero-index quantum metamaterial, creating a hot spot with concentrated probability current and interaction capability. On the contrary, panel (b) demonstrates the inverse transformation, from a tightly focused Gaussian beam into a plane wave. In both cases, the beams are incident from the left.

a very large (12 de Broglie wavelengths) GaAs obstacle in the center of the quantum metamaterial. In spite of the presence of this large quantum well, the tunneling phenomenon is unaffected, demonstrating the attractive cloaking capabilities of the material.

In addition to routing and cloaking, near-zero index quantum metamaterials may enable new control over the phase of electronic wave functions, making possible a variety of applications based on phase-front shaping and patterning. As basic examples, consider the focusing and defocusing of ballistic electrons, demonstrated in Fig. 5. Because the wave function of an electron at the Dirac energy does not experience any phase change, we can expect a quasistatic envelope field distribution over the entire volume of the metamaterial. By tailoring the shape of the output surface of a near-zero index material, it is therefore possible to completely manipulate the phase front at the exit. In Fig. 5(a) we show that electronic focusing can be achieved with a curved lens with near-zero quantum index, creating a hot spot with highest probability of presence for the electron. An interacting object may be placed at the focus to benefit from the enhanced interaction probability at this location. The opposite effect is demonstrated in Fig. 5(b) where a tightly focused Gaussian beam, incident from the left, is transformed into plane waves by a slab with near-zero quantum index. This exceptional capability to tame electron momentum at the nanoscale may be very interesting in nanoelectronic devices and sensing applications.

IV. CONCLUSIONS

To conclude, we have shown that metamaterials-related concepts can inspire a wealth of interesting possibilities in the realm of nanoelectronics. In this paper, we have specifically focused our attention on impedance-matched, zero-index quantum superlattices. Our design is based on a simple GaAs/AlAs superlattice that is tailored to induce a Dirac cone at the center of the Brillouin zone by accidental degeneracy of the Bloch eigenmodes. We have demonstrated that such a structure exhibits a zero quantum index of refraction at the Dirac energy and is almost perfectly matched to the AlAs substrate, making it an ideal building material in integrated nanoelectronic components. As an example of the dramatic tunneling and phase-front shaping abilities of such an artificial material, we have demonstrated its ability to connect quantum wires regardless of the bend and twist of a junction. In addition, near-zero index electronic metamaterials show considerable potential for controlling electronic momentum, as we pointed out with the instance of zero quantum index electronic lenses for focusing and defocusing ballistic electron beams.

ACKNOWLEDGMENT

This works has been supported by AFOSR Grant No. FA9550-13-1-0204 and DTRA YIP Award No. HDTRA1-12-1-0022.

[1] A. Sihvola, S. Tretyakov, and A. de Baas, J. Commun. Technol. Electron. **52**, 986 (2007).
[2] D. R. Smith, J. B. Pendry, and M. C. K. Wiltshire, Science **305**, 788 (2004).
[3] N. Engheta, Science **340**, 286 (2013).
[4] A. Alù, M. G. Silveirinha, A. Salandrino, and N. Engheta, Phys. Rev. B **75**, 155410 (2007).
[5] M. Silveirinha and N. Engheta, Phys. Rev. Lett. **97**, 157403 (2006).
[6] A. Alù, M. G. Silveirinha, and N. Engheta, Phys. Rev. E **78**, 016604 (2008).
[7] R. W. Ziolkowski, Phys. Rev. E **70**, 046608 (2004).
[8] A. Alù and N. Engheta, IEEE Trans. Antennas Propag. **58**, 2328 (2010).
[9] R. Liu, Q. Cheng, T. Hand, J. J. Mock, T. J. Cui, S. A. Cummer, and D. R. Smith, Phys. Rev. Lett. **100**, 023903 (2008).
[10] B. Edwards, A. Alù, M. E. Young, M. Silveirinha, and N. Engheta, Phys. Rev. Lett. **100**, 033903 (2008).
[11] E. J. R. Vesseur, T. Coenen, H. Caglayan, N. Engheta, and A. Polman, Phys. Rev. Lett. **110**, 013902 (2013).
[12] R. Fleury and A. Alù, Phys. Rev. B **87**, 201101 (2013).
[13] X. Huang, Y. Lai, Z. H. Hang, H. Zheng, and C. T. Chan, Nat. Mater. **10**, 582 (2011).
[14] R. Fleury and A. Alù, Phys. Rev. Lett. **111**, 055501 (2013).
[15] P. B. Catrysse, G. Veronis, H. Shin, J. T. Shen, and S. Fan, Appl. Phys. Lett. **88**, 31101 (2006); M. Choi, S. H. Lee, Y. Kim, S. B. Kang, J. Shin, M. H. Kwak, K.-Y. Kang, Y.-H. Lee, N. Park, and B. Min, Nature **470**, 369 (2011).
[16] J. B. Pendry, Phys. Rev. Lett. **85**, 3966 (2000).
[17] S. Zhang, W. Fan, N. C. Panoiu, K. J. Malloy, R. M. Osgood, and S. R. J. Brueck, Phys. Rev. Lett. **95**, 137404 (2005).
[18] Y. Zhao, M. A. Belkin, and A. Alù, Nat. Commun. **3**, 870 (2012).
[19] R. Fleury, D. L. Sounas, C. F. Sieck, M. R. Haberman, and A. Alù, Science **343**, 516 (2014).
[20] D. L. Sounas and A. Alù, ACS Photon. **1**, 198 (2014).
[21] A. Alù and N. Engheta, Phys. Rev. Lett. **103**, 043902 (2009).
[22] A. Alù and N. Engheta, Phys. Rev. E **72**, 016623 (2005); Phys. Rev. Lett. **100**, 113901 (2008).
[23] D. Rainwater, A. Kerkhoff, K. Melin, J. C. Soric, G. Moreno, and A. Alù, New J. Phys. **14**, 013054 (2012).
[24] D. Schurig, J. J. Mock, B. J. Justice, S. A. Cummer, J. B. Pendry, A. F. Starr, and D. R. Smith, Science **314**, 977 (2006).
[25] N. Landy and D. R. Smith, Nat. Mater. **11**, 25 (2013).
[26] R. Fleury, J. Soric, and A. Alù, Phys. Rev. B **89**, 045122 (2014).
[27] R. Fleury and A. Alù, FERMAT **1**, 7 (2014).
[28] J. D. Joannopoulos, S. G. Johnson, J. N. Winn, and R. D. Meade, *Photonic Crystals: Molding the Flow of Light* (Princeton University Press, Princeton, NJ, 2008).
[29] R. Fleury and A. Alù, Appl. Phys. A **109**, 781 (2012).
[30] L. Esaki and R. Tsu, IBM J. Res. Dev. **14**, 61 (1970).
[31] Y. Zhang, B. Fluegel, and A. Mascarenhas, Phys. Rev. Lett. **91**, 157404 (2003).
[32] V. V. Cheianov, V. Fal'ko, and B. L. Altshuler, Science **315**, 1252 (2007).
[33] M. G. Silveirinha and N. Engheta, Phys. Rev. Lett. **110**, 213902 (2013).
[34] I. Hrebikova, L. Jelinek, J. Voves, and J. D. Baena, Phot. Nano. Fund. Appl. **12**, 9 (2014).

[35] S. Zhang, D. A. Genov, C. Sun, and X. Zhang, Phys. Rev. Lett. **100**, 123002 (2008).
[36] A. Greenleaf, Y. Kurylev, M. Lassas, and G. Uhlmann, Phys. Rev. Lett. **101**, 220404 (2008).
[37] D.-H. Lin, Phys. Rev. A **81**, 063640 (2010); **84**, 033624 (2011).
[38] B. Liao, M. Zebarjadi, K. Esfarjani, and G. Chen, Phys. Rev. Lett. **109**, 126806 (2012).
[39] R. Fleury and A. Alù, Phys. Rev. B **87**, 045423 (2013).
[40] R. Fleury and A. Alù, Phys. Rev. B **87**, 201106(R) (2013).
[41] B. Liao, M. Zebarjadi, K. Esfarjani, and G. Chen, Phys. Rev. B **88**, 155432 (2013).
[42] N. I. Zheludev, Science **328**, 582 (2010).
[43] A. L. Rakhmanov, A. M. Zagoskin, S. Savel'ev, and F. Nori, Phys. Rev. B **77**, 144507 (2008).
[44] M. A. Castellanos-Beltran, K. D. Irwin, G. C. Hilton, L. R. Vale, and K. W. Lehnert, Nat. Phys. **4**, 929 (2008).
[45] P. Lahteenmaki, G. S. Paraoanu, J. Hassel, and P. J. Hakonen, Proc. Natl. Acad. Sci. USA **110**, 4234 (2013).
[46] M. G. Silveirinha and N. Engheta, Phys. Rev. B **86**, 161104 (2012).
[47] M. G. Silveirinha and N. Engheta, Phys. Rev. B **89**, 085205 (2014).
[48] M. G. Silveirinha and N. Engheta, Phys. Rev. B **86**, 245302 (2012).
[49] G. Bastard, *Wave Mechanics Applied to Semiconductor Heterostructures* (Wiley, New York, 1988).
[50] F. Liu, X. Huang, and C. T. Chan, Appl. Phys. Lett. **100**, 071911 (2012).
[51] Z. Liang and J. Li, Phys. Rev. Lett. **108**, 114301 (2012).
[52] K. Sakoda, Opt. Express **20**, 3898 (2012).
[53] I. Vurgaftman, J. R. Meyer, and L. R. Ram-Mohan, J. Appl. Phys. **89**, 5815 (2001).
[54] B. A. Volkov and O. A. Pankratov, Sov. Phys. JETP Lett. **42**, 178 (1985).
[55] O. A. Pankratov, S. V. Pakhomov, and B. A. Volkov, Solid State Commun. **61**, 93 (1987).
[56] J. R. Meyer, C. A. Hoffman, F. J. Bartoli, J. W. Han, J. W. Cook, J. F. Schetzina, X. Chu, J. P. Faurie, and J. N. Schulman, Phys. Rev. B **38**, 2204 (1988).
[57] S. Sone, N. Oda, T. Sasaki, and M. Kawano, J. Crystal. Growth **117**, 218 (1992).
[58] M. Gibertini, A. Singha, V. Pellegrini, M. Polini, G. Vignale, A. Pinczuk, L. N. Pfeiffer, and K. W. West, Phys. Rev. B **79**, 241406(R) (2009).
[59] D. Dragoman, J. Appl. Phys. **108**, 094302 (2010).
[60] A. N. Khondker, M. R. Khan, and A. F. M. Anwar, J. Appl. Phys. **63**, 5191 (1988).
[61] A. N. Khondker, J. Appl. Phys. **67**, 6432 (1990).
[62] M. A. Alam and A. N. Khondker, J. Appl. Phys. **68**, 6501 (1990).
[63] R. Kaji, K. Hayata, and M. Koshiba, Electron. Commun. Jpn. (Part II Electron.) **75**, 44 (1992).
[64] H. Sanada, N. Nagai, N. Ohtani, and N. Miki, Electron. Commun. Jpn. (Part II Electron.) **77**, 106 (1994).
[65] A. F. M. Anwar, A. N. Khondker, and M. R. Khan, J. Appl. Phys. **65**, 2761 (1989).
[66] N. Ohtani, N. Nagai, M. Suzuki, and N. Miki, Electron. Commun. Jpn. (Part II Electron.) **74**, 27 (1991).
[67] T. K. Gaylord and K. F. Brennan, Appl. Phys. Lett. **53**, 2047 (1988).
[68] T. K. Gaylord, E. N. Glytsis, and K. F. Brennan, J. Appl. Phys. **67**, 2623 (1990).
[69] D. M. Pozar, *Microwave Engineering* (Wiley, New York, 2011).